Eurographics Symposium on Rendering - Experimental Ideas & Implementations (2016)
E. Eisemann and E. Fiume (Editors)

A General Micro-flake Model for Predicting the Appearance of Car Paint

S. Ergun[1] and S. Önel[2] and A. Ozturk[3]

[1] The International Computer Institute, Ege University, Turkey
[2] The Department of Software Engineering, Yasar University, Turkey
[3] The Department of Computer Engineering, Izmir University, Turkey

Figure 1: *Renderings of car paints based on our micro-flake model. Left: pigment particles, Center: interference flakes, Right: mirror flakes.*

Abstract

We present an approximate model for predicting the appearance of car paint from its paint composition. Representing the appearance of car paint is not trivial because of its layered structure which is composed of anisotropic scattering media. The Radiative Transfer Equation (RTE) is commonly used to represent the multiple scattering for the underlying structures. A number of techniques including the Monte Carlo approach, the discrete ordinates, the adding-doubling method, the Eddington approximation, as well as the 2-stream and diffusion approximations have been proposed so far to improve visualization accuracy. Each of these techniques hold advantages over the others when their appropriate conditions are met. The adding-doubling method, in particular, is recognized to be computationally simple and accurate.

*Jakob et al. [JAM*10] has generalized the RTE for anisotropic scattering structures and proposed to use a micro-flake model based on double-sided specularly reflecting flakes. They also developed an anisotropic diffusion approximation to solve the corresponding RTE.*

In this paper, considering the translucent micro-flakes we proposed to use a modified version of the model which was developed by Jakob et al. We utilized the adding-doubling method instead of the diffusion-approximation for the new micro-flake model. The proposed approach also provided a good ground for data compression used in the evaluation of RTE.

Empirical comparisons have been made to assess the accuracy and computational efficiency of the proposed model. Based on the sample data, we showed that our model provides visually satisfactory results for the appearance of multi-layered car paint.

Categories and Subject Descriptors (according to ACM CCS): I.3.7 [Computer Graphics]: Three-Dimensional Graphics and Realism—Color, shading, shadowing, and texture

1. Introduction

Predicting the appearance of a product at the beginning of design phase is of great importance in many industrial applications. In this regard, accurate modeling of surface scattering becomes crucial for their commercial success. Various models have been proposed to simulate scattering surfaces of products under certain simplifying assumptions and some of them have provided accurate representations. However, as for the modern car paints, surfaces that are composed of multiple layers of scattering and absorbing media can be more complex.

So far, various models have been proposed for representing the multiple scattering for these kind of media. The Radiative Transfer Equation (RTE) has been commonly used to model the multiple scattering for both homogeneous and heterogeneous media

DOI: 10.2312/sre.20161211

whose properties assumed to be invariant under rotation or, in other words, the model is limited to isotropic medium only. Considering the anisotropic scattering structure for which the scattered intensity changes with the viewing angle and orientation of the particles, Jakob et al. [JAM*10] has generalized the RTE to allow the underlying properties of scattering medium. They employed a micro-flake model essentially similar to microfacet surface reflection models. They also derived a diffusion approximation together with a dipole BSSRDF for anisotropic translucent materials.

Generally, microfacet models do not treat micro-flakes individually but as randomly aggregated structures to represent the overall reflection behavior of the medium. Jakob et al. [JAM*10] has considered micro-flakes individually and assumed that the flakes are planar, opaque and their albedo depend only on the direction of incoming light.

Diffusion approximation technique is known to provide approximate solutions for anisotropic scattering media. In this paper, we propose to use adding-doubling technique which is known to be more accurate and computationally simpler than diffusion approximation for solving anisotropic RTE. We also modified the underlying model to handle translucent micro-flakes. Finally, we proposed to employ an efficient compression technique for evaluating the Fourier coefficients of micro-flake's reflection function.

This paper is organized in the following way: The next section summarizes the related work about the multiple scattering problem for car paint. In Section 3, we explain our modified micro-flake model in the context of anisotropic RTE. In Section 4, we describe the solution to the underlying problem using adding-doubling technique and the related compression procedures. In Section 5, we explain the application of the proposed adding-doubling technique by considering spherical pigments, mirror and interference flakes. Empirical results based on renderings and comparisons are given in Section 6. Section 7 is devoted to further discussion and future work.

2. Related work

Multiple scattering has an extensive literature in computer graphics. This section focuses on the problem of modeling the appearance of multi-layered car paint and summarizes and discusses relevant previous work.

Takagi et al. [TTOO90] simulated weather conditions using an empirical model based on measured BRDF data. Dumont-Bècle et al. [DBFK*01] proposed an interactive model that simulated gloss by assigning an environment map texture for each parameter in the paint layer. Shimizu et al. [SMW03] modified the approach of Dumont-Bècle et al. by using pre-computed environment map textures.

Ershov et al. [EKM01] presented a physical model based on paint decomposition to represent scattering of pearlescent paints. The BRDF of car paint was computed using the adding-doubling method, which was first introduced by Hansen [Han69]. In a later work, Ershov et al. [EĎKM04] used that model to develop a reverse engineering technique, which showed that the BRDF measurements can be used to determine the paint compositions.

Günther et al. [GCG*05] presented an acquisition and rendering technique for car paint by setting up an image based device. They used measured BRDF and fitted multi-lobe Cook-Torrance [CT82] model to car paint data. Rump et al. [RMS*08] proposed a hybrid method of analytical and image based representation. They represented the reflectance behavior by the Cook-Torrance BRDF model and the spatial variation by a Bidirectional Texture Function (BTF). This hybrid model simulated complex effects, including specular reflection as well as spatially varying glitter that had an illusion of depth and shifting colors. Rump et al. [RSK09] extended their work by resampling and compressing their measured BTF data to improve the compression ratio.

Kim et al. [KSKL10] presented an image-based goniospectrophotometer system to measure the spectral BRDF. They used multispectral images and high-dynamic-range images to simulate the effect of pearlescent paints. In their work they used Non-negative Matrix Factorization (NMF) technique to compress large size of measured BRDF data. Analogously Seo et al. [SKKL11] presented a data-driven approach to predict the appearance of metallic paint by using a weighted interpolation on the measured BRDF, and a compact representation of the BRDF data was introduced.

Ferrero et al. [FRC*13] described characterization of colors in special-effect coatings by analyzing the spectral BRDF, and a procedure was introduced to predict the color of the coatings at any geometry.

Ďurikovič et al. [ĎM13] described an image synthesizing procedure which used measured spectral BRDF. They also simulated the sparkling effect by using sparkle textures which were captured by processing multiple photographs under different incident light directions.

Jakob et al. [JdJM14] have developed a general solution for simulating scattering from isotropic and anisotropic layered surfaces. Using their approach, they managed to represent accurately BSDFs for a wide range of layered structures. A general solution was found by Jakob et al. [JdJM14] which simulated layered isotropic and anisotropic scattering patterns. While using it, it is possible to accurately represent a wide range of layered BSDF structures.

3. A Micro-flake model used in Anisotropic Radiative Transfer Equation

Generally, car paint is composed of four layers, a clearcoat, basecoat, and primer and substrate layers, as shown in Figure 2. The clearcoat is a homogeneous layer that is made of transparent binder. It is the main source of specular reflection. The basecoat is a transparent binder with embedded mirror flakes, interference flakes and pigments. The primer layer absorbs the scatterings of the microscopic particles. The bottom substrate layer has no reflective effect, and it is usually ignored in simulations. [KSKL10]

The paint's overall appearance is created by multiple scattering caused by microscopic particles dispersed in the basecoat. Incident light reaches these particles and is absorbed, scattered or reflected at various angles. Mirror flakes reflect certain wavelengths, while they absorb others. Interference flakes, which are mostly translu-

cent and coated with a thin film, cause light to interfere with itself. This interference cancels or amplifies certain wavelengths of incoming light. Since the interference depends on the incident direction, reflected wavelengths changes accordingly, thus resulting in a pearlescent appearance.

The RTE is commonly used to model isotropic media. However, the reflectance of the micro-flakes changes depending on their orientations and the resulting scattering changes with the scattering angle. Therefore, the RTE needs to be modified in order to provide an adequate representation of anisotropic media. Jakob et al. [JAM*10] proposed the following modification of the RTE to model the scattering for anisotropic medium:

$$(\vec{\omega}\cdot\nabla)L(\vec{\omega})+\sigma_t(\vec{\omega})L(\vec{\omega}) = \sigma_s(\vec{\omega})\int_{S^2} f_p(\vec{\omega}'\to\vec{\omega})L(\vec{\omega}')\,d\vec{\omega}'+Q(\vec{\omega}), \quad (1)$$

where, L represents the radiance distribution, f_p is the phase function, and σ_t and σ_s are the attenuation and scattering coefficients respectively. $\vec{\omega}'$ and $\vec{\omega}$ are the incoming and outgoing light directions consecutively and Q stands for the volume source. The main differences between isotropic and anisotropic RTEs are that the anisotropic ones have attenuation and scattering coefficients which depend on the light's direction. Also, the phase function of anisotropic RTE not only depends on the angle between incoming and outgoing directions, but also on the orientation of the particles.

Jakob et al. [JAM*10] proposed a micro-flake model that can be used in this framework to simulate opaque flakes. We reconfigured that model to represent the interference effects of translucent flakes. The original equation has been modified under the assumption that a certain amount of light is transmitted through the flake:

$$\begin{aligned}\sigma_s(\vec{\omega}) &= a\rho\int_{S^2} R(|\vec{\omega}\cdot\vec{m}|)\,|\vec{\omega}\cdot\vec{m}|\,D(\vec{m})\,d\vec{m}\\ \sigma_t(\vec{\omega}) &= a\rho\int_{S^2} (1-T(|\vec{\omega}\cdot\vec{m}|))\,|\vec{\omega}\cdot\vec{m}|\,D(\vec{m})\,d\vec{m}\\ f_p(\vec{\omega}'\to\vec{\omega}) &= \frac{a\rho}{4\sigma_s(\vec{\omega})}R(|\vec{\omega}'\cdot h(\vec{\omega},-\vec{\omega}')|)\\ &\quad (D(h(\vec{\omega},-\vec{\omega}'))+D(-h(\vec{\omega},-\vec{\omega}'))) \quad (2)\end{aligned}$$

where, a is the surface area of the flake, ρ stands for the density of flakes per unit volume, R and T represent the reflectance and transmittance functions of the flake, D is the probability density function of flake normals defined on a sphere, $\vec{\omega}'$ and $\vec{\omega}$ are the incident and scattered light directions, and h denotes the halfway vector. The incident direction of the phase function points inward to the paint layer. For this reason, the $\vec{\omega}'$ direction has to be flipped so that the halfway vector can be calculated. Note that $R+T$ is always less than or equal to 1 due to the conservation of energy law. In the case when $T=0$, the above equations reduce to equations of Jakob et al. [JAM*10] for opaque flakes.

4. A solution for the RTE using the proposed micro-flake model

The RTE is the generalization of scattering events which defines the behavior of light in a participating medium. Several methods

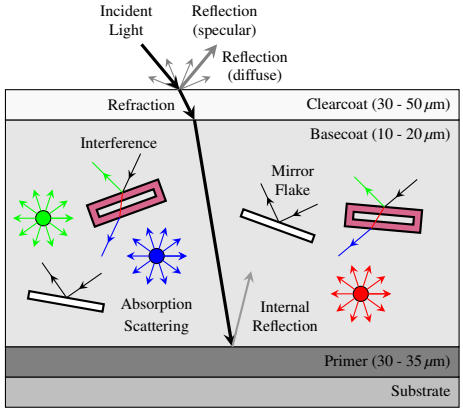

Figure 2: *The paint structure*

have been developed to solve the RTE including approximate methods (Eddington [JAV05], 2-stream [JAV05], and diffusion [KJ03]) and accurate methods (the Monte Carlo [RK99], discrete ordinates [STWJ88], and adding-doubling [EKM01]). Although approximate methods are known to be computationally more efficient then the accurate methods, they do not converge asymptotically. However, accurate methods are asymptotically convergent and preferred in most industrial applications, despite their higher computational costs.

Our micro-flake model can be used with one of the accurate methods mentioned above. We proceeded to use the adding-doubling approach, which provides an exact solution to the RTE. The adding-doubling method slices each layer into very thin imaginary sublayers in which multiple scattering can be neglected. The scattering operators R_τ and T_τ are calculated for each of these thin sublayers as follows:

$$\begin{aligned}R_\tau(\mu,\mu',\phi) &= \frac{\tau a\rho}{4\mu}R(\mu,\mu',\phi)\left(D(h(\mu,\mu',\phi))+D(-h(\mu,\mu',\phi))\right)\\ T_\tau(\mu,\mu',\phi) &= \delta_{\mu\mu'}\delta_{0\phi}\left(1-\frac{\tau}{\mu}\sigma_t(\mu)\right)+R_\tau(\mu,\mu',\phi) \quad (3)\end{aligned}$$

where τ represents the optical depth, δ symbolizes the Kronecker delta, and μ' and μ stands for the cosine of the elevation angles for incoming and outgoing light directions respectively. Other parameters are defined as in Eq. 2. After the reflectance and transmissions are calculated for a thin layer, they are doubled recursively until the desired thickness is achieved. The scattering operators are calculated for the layers and the Fresnel boundaries. Then, the whole coat's scattering operators are calculated with the adding method. This process is illustrated in Figure 3. Clearly, the adding-doubling method has easy mathematical operations for solving the RTE.

To compute the outgoing radiance using the adding-doubling method, we first discretize the functions and represent them in a different basis. Chandrasekhar [Cha60] proposed to discretize the light distribution at the depth τ by using a Fourier series in the azimuth angle ϕ and point samples in the cosines of the elevation angle [JAM*10]. In this parameterization, radiance functions are represented by scattering matrices. Using adding equations, the scat-

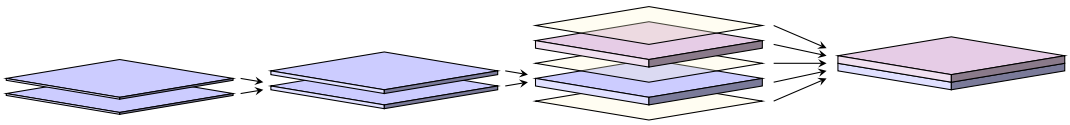

Figure 3: *The Adding-Doubling Method [JdJM14]. Thin slices are combined to generate layers, and different layers are merged with Fresnel boundaries to form the paint.*

tering matrix of a composite layer is computed from the distinct paint layers' matrices. Assuming that we know the scattering matrices of two adjacent layers, we can use the following equations to compute the scattering matrix of the resulting composite layer.

$$\begin{aligned}
\tilde{\mathbf{R}}^t &= \mathbf{R}_1^t + \mathbf{T}_1^{bt}\left(\mathbf{I}-\mathbf{R}_2^t\mathbf{R}_1^b\right)^{-1}\mathbf{R}_2^t\mathbf{T}_1^{tb}\\
\tilde{\mathbf{R}}^b &= \mathbf{R}_2^b + \mathbf{T}_2^{tb}\left(\mathbf{I}-\mathbf{R}_1^b\mathbf{R}_2^t\right)^{-1}\mathbf{R}_1^b\mathbf{T}_2^{bt}\\
\tilde{\mathbf{T}}^{tb} &= \mathbf{T}_2^{tb}\left(\mathbf{I}-\mathbf{R}_1^b\mathbf{R}_2^t\right)^{-1}\mathbf{T}_1^{tb}\\
\tilde{\mathbf{T}}^{bt} &= \mathbf{T}_1^{bt}\left(\mathbf{I}-\mathbf{R}_2^t\mathbf{R}_1^b\right)^{-1}\mathbf{T}_2^{bt}
\end{aligned} \tag{4}$$

where the R_i^t and R_i^b are i^{th} layer's reflections from the top and from the bottom; T_i^{tb} and T_i^{bt} are the transmissions from top to bottom and bottom to top respectively. The above formulae can be applied iteratively to combine several layers according to material's structure.

Consecutive layers of different refractive indices make light reflect and refract at their boundaries. Therefore, a Fresnel boundary between these layers should also be applied.

To represent the reflectance and transmittance functions introduced in Eq. 3, in the basis of Chandrasekhar, Fourier projections of R_τ as a function of the azimuthal angle should be calculated. By the convolution theorem it is sufficient to compute the Fourier projections of R and D separately.

An important issue in modeling micro-flakes is to determine the distribution of flake normals. A number of multi-variate distributions have been proposed to represent the flake normal distributions. Beckmann distribution is commonly used in reflectance models [CT82]. In this paper we proceed to use Beckmann distribution also because of its flexibility and generality. Assuming that the distribution of flake normals follow a Beckmann distribution with parameter α given as:

$$f(\cos\theta) = \frac{1}{2\pi\alpha^2\left|\cos\theta\right|^3}e^{-\tan^2\theta/\alpha^2} \tag{5}$$

then the distribution of flake normals can be expressed as

$$\begin{aligned}
D\left(h\left(\mu,\mu',\phi\right)\right) &= D\left(-h\left(\mu,\mu',\phi\right)\right)\\
&= \frac{2^{1/2}f_{rem}(\phi)\exp\left(A+B\cos\phi\right)}{\alpha^2\pi\left|\mu-\mu'\right|^3}
\end{aligned} \tag{6}$$

where,

$$\begin{aligned}
f_{rem}(\phi) &= \left(1-\mu\mu'-\sqrt{\left(1-\mu^2\right)\left(1-\mu'^2\right)}\cos\phi\right)^{3/2}\\
A &= \left(\mu^2+\mu'^2-2\right)/\left(\alpha^2\left(\mu-\mu'\right)^2\right)\\
B &= 2\left[\left(1-\mu^2\right)\left(1-\mu'^2\right)\right]^{1/2}/\left[\alpha^2\left(\mu-\mu'\right)^2\right]
\end{aligned} \tag{7}$$

Computation of Fourier expansion of this distribution can be obtained as described in [JdJM14]. Jakob et al. [JdJM14] proposed to use a similar distribution function to this one and calculated its Fourier expansion. In their implementation a different f_{rem} function was used. We utilized that same strategy to compute the Fourier expansion of the probability distribution of flake normals as shown in Eq. 6.

Since the reflectance function R is defined differently for each type of particle, calculating each Fourier expansion requires extensive computations. We discretized the reflectance function in three dimensions which are represented by μ,μ' and ϕ, and sampled them in this new discrete space. For each pair (μ,μ'), the Discrete Fourier Transform (DFT) is applied to f_{rem} function over the azimuth angle ϕ. We computed the Fourier series once and stored the coefficients in a file to avoid repeated computations. To reduce the size of the stored data, we reorganized this three dimensional data for the reflectance function R within a two dimensional matrix in terms of (μ,μ') and ϕ. The size of this matrix is $n^2\times m$ where n and m are the number of elevational and azimuthal samples respectively. This matrix is factorized as a product of two matrices with respective dimensions $n^2\times r$ and $r\times m$ (where $r\ll m$). Two factorization methods, the Non-negative Matrix Factorization (NMF) [LS99] and the Singular Value Decomposition (SVD) are used to factorize this matrix. Mean relative errors with respect to the number of coefficients used in this factorization, are shown in Figure 4. As seen in the figure, the NMF fails to converge to a solution. For this reason, we employed SVD technique for matrix factorization. To enforce non-negativity we applied the square root transformation to the el-

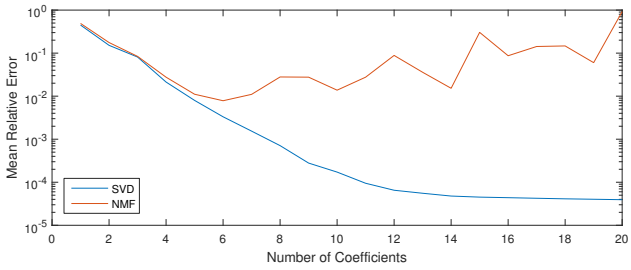

Figure 4: *Mean relative error for SVD and NMF*

ements of the reflectance matrix. In order to calculate the Fourier coefficients of the function R, each column's DFT in the second matrix (which depends only on ϕ) is used. Then, the final coefficients of the Fourier series for R is calculated by a simple matrix multiplication.

5. Implementation

Our micro-flake model can be used for any type of particles. We represented spherical pigments, mirror flakes and interference flakes using our translucent micro-flake model. By carefully modifying the reflectance function and selecting a suitable distribution of flake normals, pigments also can be simulated to behave like micro-flakes.

In this paper, we simulated pigments by using uniform distribution for flake normals and defining the reflectance function as:

$$R\left(\mu,\mu',\phi\right) = 8\pi\sigma_s g\left(\mu,\mu',\phi\right), \tag{8}$$

where, σ_s is the scattering cross section, and g is the phase function of the spherical pigment. Mie Scattering or Rayleigh approximation can be used to calculate σ_s and g. The Rayleigh scattering provides more efficient approximation than Mie Scattering when small particles are involved. However, most pigments have larger diameters than visible light's wavelength. For this reason, we opted to use the Mie Scattering theory. Evaluation of Mie phase function requires the calculation of Riccati-Bessel functions which are prone to overflow problems. To overcome this problem, various algorithms have been proposed. We used Hong Du's algorithm [Du04] which can evaluate the Mie phase function robustly and efficiently.

Mirror and interference flakes are micro-flakes by nature. Both of them also align themselves to be almost parallel to the paint surface. For this reason we used the Beckmann Distribution to represent distribution of micro-flake normals. Mirror and interference flakes reflect and transmit light in a different way. Mirror flakes are solid mirrors which perfectly reflect certain wavelengths and absorb the rest, while interference flakes selectively reflects and transmit certain wavelengths, depending on the incident light direction. Interference flakes are translucent platelets which are coated with different materials. As light is transmitted and reflected through these coats, a constructive or destructive interference occurs. This interference diminishes certain wavelengths of light, while others are amplified, changing the perceived color depending on the incident angle. The overall reflection and transmission with interference effects can be calculated efficiently by using the Transfer-Matrix method [BW99]. For a layered medium (in our case the interference flake) we calculate the wavelength dependent reflectance R_λ and transmittance T_λ for each wavelength value λ at uniformly spaced interval. These relative spectral power distributions are then used to calculate the tristimulus (CIE XYZ) and the RGB values for reflectance and transmittance functions R and T in Eq. 2.

Translucency should also be considered when modeling reflectance of interference flakes. Since, the normals of micro-flakes are nearly parallel to paint layers normal, most of the reflected light leaves the paint layer and the transmitted light travels deeper into the paint with increased scattering. If a reflective substrate layer is used or the interference flakes are mixed with other pigments, the transmitted light can travel back to the surface. The perceived diffuse color of the paint will be different from the specular color because of the color difference between the reflected and transmitted light.

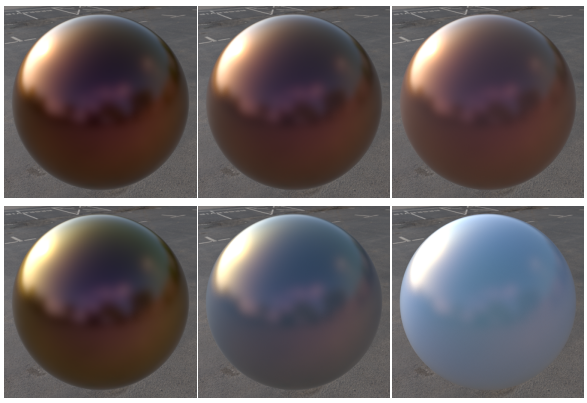

Figure 5: *The translucency effect of interference flakes coated with TiO_2. Top row: opaque micro-flakes. Bottom row: translucent micro-flakes. Columns left to right: black, gray and white primers*

In order to address the importance of generalization of the micro-flake model, we obtained renderings of spheres based on opaque and translucent flakes and the results are shown in Figure 5. Spheres on the top and bottom rows correspond to opaque flakes and translucent flakes respectively. The first, second and third columns correspond to black, gray and white primers. The effect of including translucency in the micro-flake model is clearly observed from this illustration.

6. Results

We have implemented our adding-doubling approach for the micro-flake model in the open source renderer, Mitsuba [Jak10], using Layerlab [Jak15] as a framework for our adding-doubling calculations. All the experiments described in this section were tested on a platform with Intel Xeon X5650 CPU and 48 GBs of memory.

For different types of particles, we measured the running times of compression and adding-doubling stages of the proposed method. To compare the effect of compression on running time, both raw and compressed data was used in the adding-doubling stage. Results for 6 different particles are shown in Table 1. In this table, the first two particles, which are *metallic* and *pearlescent* are interference flakes. *Metallic* particles are made up of aluminum platelets coated with magnesium fluoride, and *pearlescent* particles are composed of silica platelets coated with titanium dioxide. *Gray mirror* particles are mirror flakes that have a gray albedo. Finally *cadmium yellow (CdS)*, *titanium white (TiO_2)* and *iron black (Fe_3O_4)* pigments are inorganic and spherical.

As seen from the table, the compression procedure takes a considerable amount of time. However, compressed data is calculated

Particle	Compression	Adding-doubling (raw data)	Adding-doubling (compressed data)
Metallic	13.20 sec	6.82 sec	4.43 sec
Pearlescent	13.17 sec	7.99 sec	4.35 sec
Gray Mirror	26.53 sec	5.39 sec	4.38 sec
Cadmium Yellow	13.23 sec	9.65 sec	3.86 sec
Titanium White	13.18 sec	12.50 sec	6.17 sec
Iron Black	13.32 sec	8.28 sec	2.84 sec

Table 1: *The running times of several adding-doubling stages for different particle types. Even though compressions takes considerably longer, they are calculated only once and they reduce the amount of time spent in the adding-doubling process.*

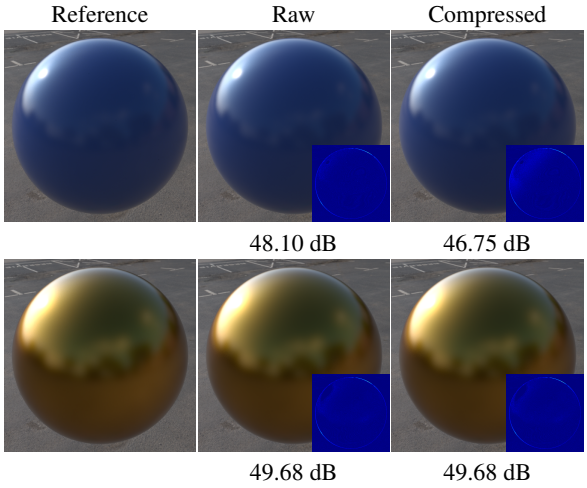

Figure 6: *Visual quality comparison of our micro-flake method. Top row: pigment particles, Bottom row: mirror flakes. first column: Path tracing, middle column: micro-flake model using raw data, last column: micro-flake model using compressed data. Insets show the differences between the corresponding images and the reference image scaled by 8 and the PSNR values are given below each image.*

only once for each particle type, and can be reused for other distributions and particle densities. Clearly, the adding-doubling procedure takes less time when compressed data is used.

The reflectance function R, described in Section 4 requires the calculation of its n^2m Fourier coefficients. However SVD needs to store only two matrices with $n^2 \times k$ and $k \times m$ dimensions, where $k = (r^2 + r)/2$, and r represent the number of coefficients. The storage requirement of the compressed data can then be calculated as $k(n^2 + m)$. Figure 4 illustrates the mean relative errors versus the number of coefficients. The choice of $r = 8$ provided visually satisfactory results in the corresponding rendered images. Based on Figure 4, we empirically concluded that $r = 8$ is sufficient. For double-precision floating points, $n = m = 200$ and $r = 8$ raw data requires 61.04 MBs of storage space for each color channel, whereas compressed data requires only 11.04 MBs of storage space. The compression ratio for this setup is 1:5.53.

In order to compare the visual quality of the proposed approach, multiple scattering of pigment particles and mirror flakes were rendered by a Monte Carlo simulation. Images were created by path tracing, and used as references. Rayleigh scattering and the micro-flake phase function that was proposed by Jakob et al. [JAM*10] were used to represent the light scattering for pigment particles and mirror flakes respectively. Using the same particles, test images were created with our micro-flake model. Results are shown in Figure 6 where rendered reference spheres are shown in the first column, and spheres based on raw and compressed data are shown in the second and third columns. The first and second rows in the figure illustrate pigment particles and mirror flakes consecutively. The corresponding PSNR values are also shown below each image. It is seen from the figure that our method produces high quality images for both particle types and data compression does not significantly change the quality of the images significantly.

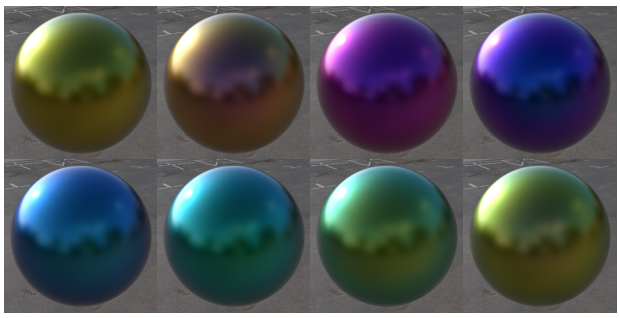

Figure 7: *Spheres rendered with interference flakes consisting of silica platelets coated with various thicknesses of TiO_2. Thickness changes from 70 nm to 140 nm (10 nm steps) from left to right, top to bottom.*

The sphere renderings in Figure 7 are based on interference flakes which are made up of silica platelets coated with TiO_2 of various thicknesses.

Finally, we rendered a car model using our flake model. Results are shown in Figure 1 where pigment particles, interference flakes and mirror flakes were used.

7. Discussion and future work

Our approach was based on the traditional adding-doubling approach in which the sparkle, polarization and diffraction effects of light were ignored. However, these effects are important in modeling the appearance of car paint. We plan to extend our approach to consider these effects and make comparisons with existing models.

Acknowledgements

This work was supported by the Scientific and Technical Research Council of Turkey (Project No: 115E458).

References

[BW99] BORN M., WOLF E.: *Principles of optics: electromagnetic theory of propagation, interference and diffraction of light*. Cambridge University Press, 1999. 5

[Cha60] CHANDRASEKHAR S.: *Radiative transfer*. Dover publications, New York, 1960. Unabridged and slightly revised version of the work first published in 1950. 3

[CT82] COOK R. L., TORRANCE K. E.: A reflectance model for computer graphics. *ACM Trans. Graph. 1*, 1 (Jan. 1982), 7–24. 2, 4

[DBFK*01] DUMONT-BÈCLE P., FERLEY E., KEMENY A., MICHELIN S., ARQUÈS D.: Multi-texturing approach for paint appearance simulation on virtual vehicles. In *Proceedings of the driving simulation conference* (2001), pp. 123–133. 2

[ĎM13] ĎURIKOVIČ R., MIHÁLIK A.: Metallic paint appearance measurement and rendering. *Journal of Applied Mathematics, Statistics and Informatics 9*, 2 (2013), 25–39. 2

[Du04] DU H.: Mie-scattering calculation. *Appl. Opt. 43*, 9 (Mar 2004), 1951–1956. 5

[EĎKM04] ERSHOV S., ĎURIKOVIČ R., KOLCHIN K., MYSZKOWSKI K.: Reverse engineering approach to appearance-based design of metallic and pearlescent paints. *The Visual Computer 20*, 8-9 (2004), 586–600. 2

[EKM01] ERSHOV S., KOLCHIN K., MYSZKOWSKI K.: Rendering pearlescent appearance based on paint-composition modelling. *Comput. Graph. Forum 20*, 3 (2001), 227–238. 2, 3

[FRC*13] FERRERO A., RABAL A., CAMPOS J., MARTÍNEZ-VERDÚ F., CHORRO E., PERALES E., PONS A., HERNANZ M. L.: Spectral brdf-based determination of proper measurement geometries to characterize color shift of special effect coatings. *J. Opt. Soc. Am. A 30*, 2 (Feb 2013), 206–214. 2

[GCG*05] GÜNTHER J., CHEN T., GOESELE M., WALD I., SEIDEL H.-P.: Efficient acquisition and realistic rendering of car paint. In *Proceedings of 10th International Fall Workshop - Vision, Modeling, and Visualization (VMV) 2005* (Nov. 2005), Greiner G., Hornegger J., Niemann H., Stamminger M., (Eds.), Akademische Verlagsgesellschaft Aka GmbH, pp. 487–494. 2

[Han69] HANSEN J. E.: Radiative transfer by doubling very thin layers. *Astrophysical Journal 155* (Feb. 1969), 565–573. 2

[Jak10] JAKOB W.: Mitsuba renderer, 2010. http://www.mitsuba-renderer.org. 5

[Jak15] JAKOB W.: layerlab: A computational toolbox for layered materials. In *SIGGRAPH 2015 Courses* (New York, NY, USA, 2015), SIGGRAPH '15, ACM. 5

[JAM*10] JAKOB W., ARBREE A., MOON J. T., BALA K., MARSCHNER S.: A radiative transfer framework for rendering materials with anisotropic structure. *ACM Trans. Graph. 29*, 4 (July 2010), 53:1–53:13. 1, 2, 3, 6

[JAV05] JIMÉNEZ-AQUINO J., VARELA J.: Two stream approximation to radiative transfer equation: An alternative method of solution. *Revista mexicana de física 51*, 1 (2005), 82–86. 3

[JdJM14] JAKOB W., D'EON E., JAKOB O., MARSCHNER S.: A comprehensive framework for rendering layered materials. *ACM Trans. Graph. 33*, 4 (July 2014), 118:1–118:14. 2, 4

[KJ03] KHAN T., JIANG H.: A new diffusion approximation to the radiative transfer equation for scattering media with spatially varying refractive indices. *Journal of Optics A: Pure and Applied Optics 5*, 2 (2003), 137. 3

[KSKL10] KIM D. B., SEO M. K., KIM K. Y., LEE K. H.: Acquisition and representation of pearlescent paints using an image-based goniospectrophotometer. *Optical engineering 49*, 4 (2010), 043604–043604. 2

[LS99] LEE D. D., SEUNG H. S.: Learning the parts of objects by non-negative matrix factorization. *Nature 401*, 6755 (Oct. 1999), 788–791. 4

[RK99] ROBERTI L., KUMMEROW C.: Monte carlo calculations of polarized microwave radiation emerging from cloud structures. *Journal of Geophysical Research: Atmospheres 104*, D2 (1999), 2093–2104. 3

[RMS*08] RUMP M., MÜLLER G., SARLETTE R., KOCH D., KLEIN R.: Photo-realistic rendering of metallic car paint from image-based measurements. *Computer Graphics Forum 27*, 2 (Apr. 2008), 527–536. 2

[RSK09] RUMP M., SARLETTE R., KLEIN R.: Efficient resampling, compression and rendering of metallic and pearlescent paint. In *Vision, Modeling, and Visualization* (Nov. 2009), Magnor M., Rosenhahn B., Theisel H., (Eds.), pp. 11–18. 2

[SKKL11] SEO M. K., KIM K. Y., KIM D. B., LEE K. H.: Efficient representation of bidirectional reflectance distribution functions for metallic paints considering manufacturing parameters. *Optical Engineering 50*, 1 (2011), 013603–013603–12. 2

[SMW03] SHIMIZU C., MEYER G. W., WINGARD J. P.: Interactive goniochromatic color design. In *Color Imaging Conference* (2003), IS&T - The Society for Imaging Science and Technology, pp. 16–22. 2

[STWJ88] STAMNES K., TSAY S.-C., WISCOMBE W., JAYAWEERA K.: Numerically stable algorithm for discrete-ordinate-method radiative transfer in multiple scattering and emitting layered media. *Appl. Opt. 27*, 12 (Jun 1988), 2502–2509. 3

[TTOO90] TAKAGI A., TAKAOKA H., OSHIMA T., OGATA Y.: Accurate rendering technique based on colorimetric conception. *SIGGRAPH Comput. Graph. 24*, 4 (Sept. 1990), 263–272. 2